

P. Bordas · J. M. Paredes · V. Bosch-Ramon · M. Orellana

Synchrotron emission from secondary leptons in microquasar jets

Received: date / Accepted: date

Abstract We present a model to estimate the synchrotron radio emission generated in microquasar (MQ) jets due to secondary pairs created via decay of charged pions produced in proton-proton collisions between stellar wind ions and jet relativistic protons. Signatures of electrons/positrons are obtained from consistent particle energy distributions that take into account energy losses due to synchrotron and inverse Compton (IC) processes, as well as adiabatic expansion. The space parameter for the model is explored and the corresponding spectral energy distributions (SEDs) are presented. We conclude that secondary leptonic emission represents a significant though hardly dominant contribution to the total radio emission in MQs, with observational consequences that can be used to test some still unknown processes occurring in these objects as well as the nature of the matter outflowing in their jets.

Keywords microquasars · radio emission · secondary leptons

PACS 98.38.Fs · 97.80.Jp · 95.30.Cq

P. Bordas, and J. M. Paredes
Departament d'Astronomia i Meteorologia, Universitat de Barcelona,
Martí i Franquès 1, 08028, Barcelona, Spain
Tel.: +34-934039225, +34-934021130
Fax: +34-934021133
E-mail: pbordas@am.ub.es; jmparedes@ub.edu

V. Bosch-Ramon
Max Planck Institut für Kernphysik, Saupfercheckweg 1, Heidelberg
69117, Germany
Tel.: +49 6221516586
Fax: +49 6221516324
E-mail: vbosch@mpi-hd.mpg.de

M. Orellana
Instituto Argentino de Radioastronomía, CC5, (1894) Villa Elisa,
Buenos Aires, Argentina.
Tel.: +54-221-482-4903
fax: +54-221-425-4909
E-mail: morellana@irma.iar.unlp.edu.ar

1 Introduction

X-ray binary systems (XRBs) are composed by either a stellar mass black hole or a neutron star, and a normal (non degenerated) star which supplies matter to the compact object through the formation of an accretion disk. Some 260 XRBs are known up to now [1] probably corresponding to an underlying population of some tens of thousands of compact objects in our Galaxy. A few of these sources present also non-thermal radio emission, hence evidencing the existence of mechanism(s) capable of injecting and/or accelerating large numbers of relativistic particles. Some radio emitting X-ray binary systems (REXBs) have been observed showing ejection of material at relativistic velocities and to display jets like those seen in quasars and active galactic nuclei but at $\sim 10^{-6}$ times shorter scales. This analogy is the reason for calling them microquasars (MQs) [2] and making them some of the most interesting objects for astrophysics. Furthermore, attention on these objects has grown since the proposal of Paredes et al. (2000) [3] of MQs as counterparts of some of the unidentified gamma-ray sources of the EGRET catalog [4] and hence pointing them as plausible high energy emitters. A strong confirmation of this association has come from the detections of the MQs LS 5039 and LS I +61 303 at TeV energies using respectively the ground-based Cherenkov telescopes HESS [5] and MAGIC [6], giving support and empowering at the same time a number of previous detailed studies centered on the mechanisms operating in these sources in order to explain the gamma ray domain (see, e.g., [7] and [8]). Moreover, a jet origin of the emission from MQs has been suggested from the observation of synchrotron emission of relativistic electrons/positrons extending from the radio all the way into the X-ray regime. In this sense jet-like models have focused on different approaches regarding the particle origin that could generate the required emission properties in a consistent way. Some of them consider leptons directly injected at the base of the jet and, in extending outwards, Compton-interaction with external/self-created photon fields produces high energy radiation. Other models deal with an hadronic origin of the

high energy emission, through proton-proton interactions and pion decay producing gamma rays and leaving the resulting co-generated leptons as low energy emitters. The present work refers to the later procedure, focusing on the modelisation of the secondary leptonic synchrotron emission in order to constrain the characterization of MQ jets. An outline of the model is given in the next, followed by the results showing the SEDs and lightcurves under different parameter assumptions and the conclusions that can be extracted from them.

2 Model description

We have taken a binary system formed by a black hole and a high-mass early-type star which feeds the accretion transfer of mass onto the compact object while developing an accretion disk. Part of the accretion power is converted to kinetic and magnetic energy of the accretion flow under the effects of the compact object potential well and a relativistic e^\pm - p plasma is ejected in a direction taken to be perpendicular to the plane defined by the accretion disk. This plane is the same as the orbital one, even if this condition can be relaxed to allow a more general situation but for simplicity we assume coplanarity in our model. Jet energetics is assumed to be dominated by accretion, and further energy sources like compact object rotation have been neglected at this stage. The jet will also contain a magnetic field B_{jet} associated with the plasma. We assume that the matter kinetic luminosity is higher than the magnetic luminosity (or total magnetic energy crossing the jet section per time unit) in the jet regions we are concerned with, although the magnetic field can be still significant once the jet is formed, since the ejection mechanism have likely a magneto-hydrodynamical origin.

In this scenario we deal with radiative processes that take place in the jet and can produce significant emission in the radio spectrum. Although the contribution of protons could still be significant from the radiative point of view, we will focus on the leptonic component only. The reader is related to other works (see, e.g., [9] and [8]) for treatments on primary hadrons.

2.1 Secondary generation

Secondary leptons are generated in p - p interactions of hot protons in the jet with the companion star wind that extends out isotropically producing charged and neutral pions (π^\pm , π^0) through the reaction channel $p + p \rightarrow p + p + \xi_{\pi^0} \pi^0 + \xi_{\pi^\pm} (\pi^+ + \pi^-)$, where $\xi_{\pi^\pm} \sim 2(E_p/GeV)^{1/4}$ is the charged pion multiplicity. The relativistic injection proton spectrum is a power law $N_p(E_p) = K_p E_p^{-\alpha}$ where $E_p^{min} \leq E_p \leq E_p^{max}$ where the constant K_p can be found normalisation to the total power that goes to protons Q_p . The corresponding proton flux will be given by $J_p(E_p) = (c/4\pi) K_p (z_0/z)^2 E_p^{-\alpha}$. We assume that a fraction of 1/10 of the matter that crosses the

Table 1 Parameter values used throughout the model.

parameter	Symbol	Value
Black hole mass	M_{bh}	$3M_\odot$
Injection point	z_0	$50R_g$
Initial radius	R_0	$5R_g$
Radius of the companion star	R_*	$15R_\odot$
Orbital radius	a	$3R_*$
Luminosity companion star	L_*	1.6×10^{39} erg/s
Mass loss rate	\dot{M}_*	$3 \cdot 10^{-6} M_\odot \text{yr}^{-1}$
Jet's Lorentz factor	Γ	1.02
Jet kinetic luminosity	Q_j	10^{36} erg/s
Proton kinetic Luminosity	Q_p	10^{35} erg/s
Minimum proton energy	E_p^{min}	2 GeV
Maximum proton energy	E_p^{max}	100 TeV
Leptonic spectral index	P	2.2
Wind-jet penetration factor	f_p	0.1
Magnetic field at z_0	B_0	$10^2, 10^3, 10^4$

jet region penetrates into it. When charged and neutral pions are created, the first will decay to muons and subsequently to electrons and positrons, while the second decays to high energy photons through

$$\begin{aligned} \pi^+ &\rightarrow \nu_\mu + \mu^+ \rightarrow \nu_\mu + e^+ + \bar{\nu}_e + \bar{\nu}_\mu \\ \pi^- &\rightarrow \bar{\nu}_\mu + \mu^- \rightarrow \bar{\nu}_\mu + e^- + \bar{\nu}_e + \nu_\mu \\ \pi^0 &\rightarrow 2\gamma. \end{aligned}$$

For an injection proton spectrum as the one given above, the pion spectrum (in the jet reference frame) will be a power law and the electron/positron distribution will also follow a power law [10] with a differential pair injection rate given by $J_e(E_e) = K_e E_e^{-P}$ where we use a value $P = 2.2$.

2.2 Secondary evolution

This injected electron-positron population suffers subsequent radiative cooling due to synchrotron and inverse Compton losses as well as adiabatic expansion given by

$$\begin{aligned} \left[\frac{dE_{e^\pm}}{dt} \right]_{sync} &= -2.36 \cdot 10^{-3} B^2 E_{e^\pm}^2, \\ \left[\frac{dE_{e^\pm}}{dt} \right]_{IC} &= -3.90 \cdot 10^{-2} U_{star} E_{e^\pm}^2, \\ \left[\frac{dE_{e^\pm}}{dt} \right]_{exp} &= \frac{2}{3} \frac{V_{exp}}{R(z)} E_{e^\pm} \end{aligned}$$

respectively. Here U_{star} is the companion star's photon field given by $U_{star} = \frac{L_*}{4\pi d^2 c}$ where d is the distance from the star and in our case $L_* = 1.6 \cdot 10^{39}$ erg/s, and $V_{exp} = dR(z)/dt$ is the lateral expansion velocity of the jet. Fresh electrons and positrons that have been injected at a certain point into the jet suffer the different energy losses modifying in this way the spectral distribution of particles at each height z . Moreover, different evolution stages sum at each height since injection of fresh particles occurs all along the jet and therefore a mix

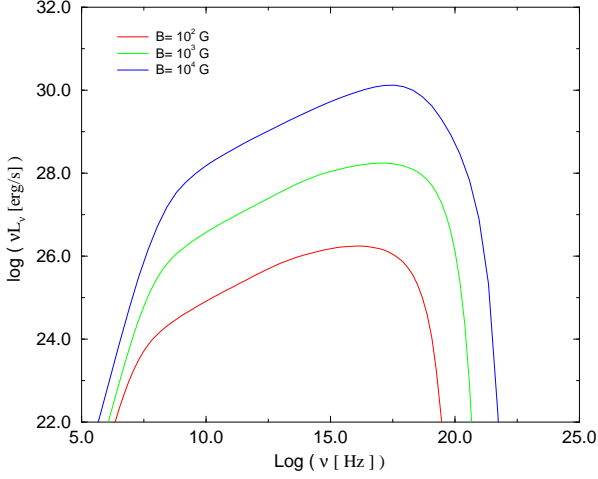


Fig. 1 The strength of the magnetic field B is treated as a free parameter in our model. Synchrotron losses will be enhanced when taking higher values for B but, since injection occurs all along the jet inside the binary system (until a distance roughly given by $z \simeq R_{orb} \sim 10^{13}$ cm), the enhancement in the final emission will prevail over losses. Here we show the SEDs for three different magnetic fields (B); values indicated are taken at the base of the jet.

of multiple evolved population of electron/positron distribution arises. To compute it in a consistent way, one has to assume the continuity equation,

$$N_{e^\pm}(E_{e^\pm}, z)dE_{e^\pm} = N_{0,e^\pm}(E_{0,e^\pm}, z_0)dE_{0,e^\pm}$$

where $N_{0,e^\pm}(E_{0,e^\pm}, z_0) = K_{0,e^\pm} E_{0,e^\pm}^{-p}$ is the initial energy spectrum for the injected particle density. Solving the equations for the evolution of the particle energy along the jet axis, one can find the spectral distribution at each slice, compute de differential luminosity at each height and finally integrate to find the total luminosity.

2.3 Secondary emission

Secondary electrons and positrons will radiate through synchrotron process since we assume the presence of a magnetic field which is tangled to the plasma and oriented randomly in direction. The resulting emission will be isotropic in the jet reference frame; to compute the expected luminosity, we have used the formulae presented in [11], where expressions for the specific emission and absorption coefficients are given by

$$\begin{aligned} \epsilon_v &= C_3 B \int_0^\infty N_{e^\pm}(E_{e^\pm}) F(x) dE_{e^\pm} \\ k_v &= -\frac{c^2}{2v^2} C_3 B \int_0^\infty E_{e^\pm}^2 \frac{d}{dE} \left(\frac{N_{e^\pm}(E_{e^\pm})}{E_{e^\pm}^2} \right) F(x) dE_{e^\pm} \end{aligned}$$

with the function $F(x)$ given by $F(x) = x \int_x^\infty K_{5/3}(z) dz$ being $K_{5/3}$ the modified second kind Bessel functions, $x \equiv \frac{v}{v_c}$ where $v_c = \frac{3e}{4\pi m_e^2 c^3} E_{e^\pm}^2 \approx 6.27 \cdot 10^{18} E_{e^\pm}^2$ Hz is the critical frequency, and the constant $C_3 \approx 1.87 \cdot 10^{-23}$ (in CGS units).

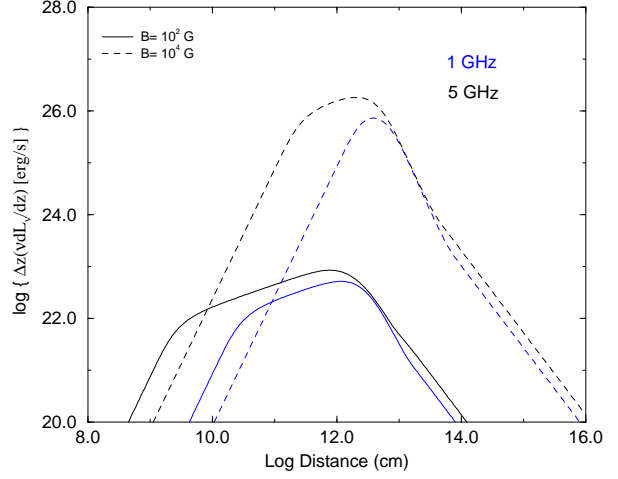


Fig. 2 Light curves of emission at 1 and 5 GHz bands at growing distances along the jet for various magnetic fields B which values are referred to the base of the jet at $z_0 = 50R_g$. Not only the overall emission but also the peak of the lightcurves moves to higher distances when increasing B , as well as the difference between the locations of the peaks for the two frequencies.

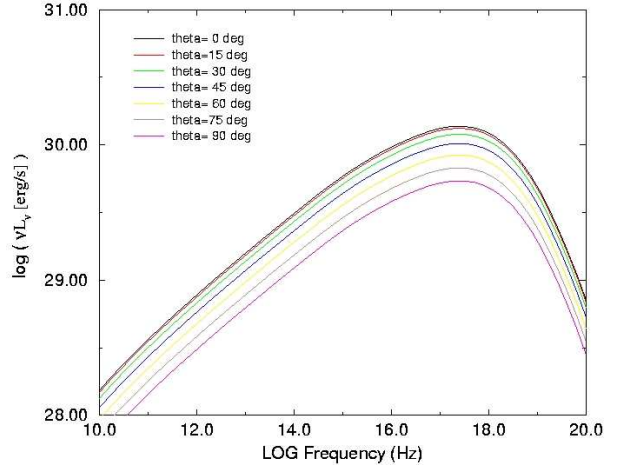


Fig. 3 Variations of the SEDs due to different observing angles θ between the approaching jet axis and the observer line of sight. As far as the jet material travels at higher velocities along the jet, the boosting will get increasingly greater while observing at smaller angles. The SEDs showed here correspond to θ ranging from 0 to $\frac{\pi}{2}$, where we have used a Lorentz factor $\Gamma \sim 1.02$ corresponding to a mildly relativistic jet with $v_j \sim 0.2c$

Then, the specific differential luminosity at a certain height z in the jet can be expressed as

$$\frac{dL_v(z)}{dz} = 2\pi R(z) \frac{\epsilon_v}{k_v} (1 - e^{-l_j k_v})$$

where l_j is the typical size of the synchrotron emitting plasma region. Now, integrating over the entire jet length we find the spectral energy distribution,

$$vL_{sync} = v \int_{z_0}^{z_{max}} \delta^2 \frac{dL_v(z)}{dz} dz$$

where $\delta = [\Gamma(1 - \beta \cos \theta_{obs})]^{-1}$ is the Doppler boosting factor.

3 Model results and conclusions

SEDs are obtained for different magnetic field values, electron/positron spectral indices and spatially distributed disks. We have estimated also the expected emission along the jet at 1 and 5 GHz. Leptons are injected in the context of hadronic secondaries generation within a detailed model that takes into account in a consistent way particle injection mechanisms and cooling due to radiation processes and adiabatic expansion. The luminosities obtained are slightly lower than in the models based on primary leptons injection, and must be considered complementary to them. However, we note that within our model there is no requirements of acceleration processes along the jet to obtain the final emission results. Such acceleration processes are still not well understood, although. They could come from diffusive shock acceleration along the jet when fresh ejecta interact with previous blobs of plasma already outflowing at lower velocities. Other scenarios assume a continuous energy transfer mechanism from the magnetic field to the matter content of the jet in such a way that the resulting parsec-scale radio emission can be explained. The fact of studying alternative models where particles are directly injected until a certain height along the jet can constrain the amount of acceleration required and contribute to the understanding of the physical mechanisms that can lead to such processes.

Signatures at different distances along the jet and specific spectral features detectable for reasonable parameter values treated in our numerical simulations have the potential to be an important clue for determining the matter content of jets. In particular, highly resolved observations at 1 and 5 GHz could determine if leptons are present at heights 10^{12-13} cm at the edge of the binary system typical region where wind matter from the companion is still significant. If electrons/positrons still show high energies due to a recent injection from hadronic interactions at these parts of the jet, it could be a signature of secondary generation without the necessity of invoking additional acceleration processes.

Acknowledgements P.B and J.M.P acknowledge support by DGI of the Spanish Ministerio de Educación y Ciencia (MEC) under grant AYA2004-07171-C02-01, as well as partial support by the European Regional Development Fund (ERDF/FEDER). V.B-R. thanks the Max-Planck-Institut für Kernphysik for its support and kind hospitality. M.O is supported by CONICET (PIP 5375) and ANPCyT (PICT 03-13291), Argentina.

References

1. Liu, Q.Z., van Paradijs, J., van den Heuvel, E.P.J.: Catalogue of high-mass X-ray binaries in the Galaxy (4th edition) *A&A*, **455**, 1165–1168 (2006)
2. Mirabel, I.F., Rodríguez, L.F.: Sources of Relativistic Jets in the Galaxy. *ARA&A*, **37**, 409–443 (1999)
3. Paredes, J.M., Martí, J., Ribó, M., Massi, M.: Discovery of a High-Energy Gamma-Ray-Emitting Persistent Microquasar. *Science* **288**, 2340–2342 (2000)
4. Hartman, R.C., Bertsch, D.L., Bloom, S.D. et al.: Third EGRET catalog (3EG), *ApJS*, **123**, 79 (1999)
5. Aharonian, F., Akhperjanian, A.G., Aye, K.M. et al.: Discovery of Very High Energy Gamma Rays Associated with an X-ray Binary. *Science* **309**, 746–749 (2005)
6. Albert, J., Aliu, E., Anderhub, H., Antoranz, P. et al.: Variable Very-High-Energy Gamma-Ray Emission from the Microquasar LS I +61 303 *Science* **312**, 1771–1773 (2006)
7. Bosch-Ramon, V., Paredes, J.M., High-energy γ -ray Emission from Microquasars: LS 5039 and LS I +61 303 *CHJAA* **5**, 133–138 (2005)
8. Romero, Gustavo E., Christiansen, Hugo R., Orellana, M.: Hadronic High-Energy Gamma-Ray Emission from the Microquasar LS I +61 303 *ApJ* **632**, Issue 2, 1093–1098 (2005)
9. Romero, G.E., Torres, D.F., Kaufman Bernadó, M., Mirabel, I.F.: Hadronic gamma-ray emission from windy microquasars, *A&A*, **410**, L1–L4 (2003)
10. Ginzburg, V.L., Syrovatskii, S.I.: The Secondary Electron Component of Cosmic Rays and the Spectrum of General Galactic Radio Emission. *Soviet Astronomy*, **8**, 342, (1964)
11. Pacholczyk, A.G.: Nonthermal processes in galactic and extragalactic sources; San Francisco, Freeman (1970)